Dynamic modelling of water-droplet spray injection in reciprocating-piston compressors

Paul Sapin[a], Michael Simpson[b], Christoph Kirmse[c] and Christos N. Markides[d]

[a] Clean Energy Processes (CEP) Laboratory, Department of Chemical Engineering, Imperial College London, London, UK, p.sapin@imperial.ac.uk
[b] Clean Energy Processes (CEP) Laboratory, Department of Chemical Engineering, Imperial College London, London, UK, m.simpson16@imperial.ac.uk
[c] Clean Energy Processes (CEP) Laboratory, Department of Chemical Engineering, Imperial College London, London, UK, c.kirmse@imperial.ac.uk
[d] Clean Energy Processes (CEP) Laboratory, Department of Chemical Engineering, Imperial College London, London, UK, c.markides@imperial.ac.uk

Abstract:

Water injection has historically been used in internal combustion engines to avoid premature ignition of the fuel-air mixture or to increase the power density of aviation engines. More recently, several innovative technologies have been developed based on injection of liquid into reciprocating-piston devices for energy conversion and storage. In the Dearman engine, liquid nitrogen is injected and rapidly evaporated by mixing with a heat transfer fluid within the cylinder to produce power. Water spray injection is also being developed for a variant of Compressed Air Energy Storage (CAES), where it is used to cool down the air during the compression process and achieve a near-isothermal compression, thus reducing both the compression work and the need for high temperature materials. Simulating the complex phenomena that take place inside a reciprocating-piston chamber during the evaporation of sprays is a time-consuming and expensive exercise in unsteady multiphase CFD. An alternative approach is presented in this paper, whereby a one-dimensional model is used to capture the overall performance of an air compressor with in-cylinder water-spray cooling. The gas phase (humid air) is considered using a zero-dimensional treatment, while the liquid water and evaporation process are handled using Lagrangian tracking. Thermo-physical properties of the humid air are derived from CoolProp. The pressure drop due to the intake and exhaust valves is calculated, as well as the unsteady heat transfer between the air-water mixture and the cylinder walls. Finally, the benefits of liquid-spray injection for CAES technologies are measured through the definition of a compression efficiency. This latter is predicted for various droplet diameters and rates of injection, and compared against a baseline (uncooled) compressor case. It is found that water-spray injection can improve the performance of CAES technologies: the maximum relative increase of the compression efficiency for the considered scenarios is 39 % (from an overall efficiency of 49.6 % for the baseline case to 68.9 % for the most efficient system).

Keywords:
Reciprocating-piston, water-spray injection, dynamic modelling.

1. Introduction

Spray injection of fluid into the chamber of a reciprocating-piston machine is a well-established technology, courtesy of a long history of fuel injection in diesel engines dating back to 1910 [1]. However, with the increasing focus on energy-efficient processes, the concept of liquid-spray injection has been adapted for several other applications, where water is the injected fluid rather than fuel.

Recent developments within the automotive industry have seen water-injection systems introduced by BMW and Bosch for petrol engines, with the aim of increasing power and fuel efficiency, and reducing CO_2 emissions [2]. Water spray is introduced into the intake manifold to cool the intake air, thereby reducing the likelihood of engine knock and allowing greater turbocharging and earlier fuel injection.

A second transport application is the Dearman engine, which uses liquid nitrogen to produce motive power [3]. Water is injected as a heat-transfer fluid to ensure rapid evaporation of the liquid nitrogen, which expands and drives the piston to produce work. The large surface area generated by a fine spray of droplets provides attractive rates of heat transfer.

For stationary applications, Coney et al. [4] have investigated a spray-cooled quasi-isothermal air compressor, reporting air temperatures below 100 °C at the compressor exit, compared to a reference temperature of 500 °C for the same pressure rise (1:25) carried out adiabatically.

Similar approaches have been proposed for isothermal compressed-air energy storage (I-CAES), in which surplus electricity is used to compress air to high pressure with minimal temperature rise. The high-pressure air can be expanded later to drive a generator. Water-spray injection is one way of achieving the high rates of heat transfer required for high power density in the compression and expansion machinery.

Qin and Loth [5] describe a liquid-piston concept for CAES with spray injection, focusing on the interphase heat and mass transfer. Putting aside valve losses, injector power, friction, and heat transfer to the cylinder walls, they showed that for the compression process alone the work required could be as little as 108 % of the isothermal work with spray injection. Fully adiabatic compression would require 141 % of the isothermal work, though this additional work is only lost if the heat of compression is rejected to ambient rather than being stored and reused.

In the present study, the major loss mechanisms within the cylinder are included alongside two-phase heat and mass transfer for the water spray. The effect of droplet diameter and mass of water injected is analysed, and the reduction in overall compression work is evaluated, compared to a baseline without spray injection.

2. Water-spray injection in reciprocating-piston compressors

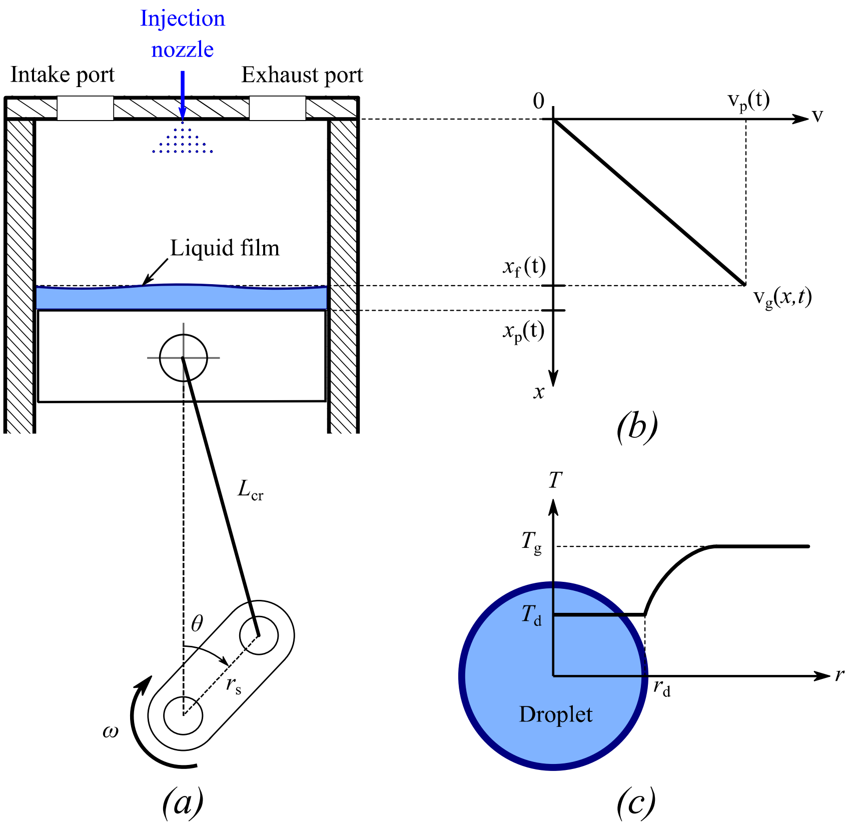

Fig. 1. a) Schematic of the reciprocating-piston compressor with a liquid (water) spray nozzle. b) Piston velocity and one-dimensional gas velocity field plotted as functions of the position along the x-axis (oriented downwards). c) Temperature profile in and near a single water droplet.

The spatial distribution of temperature, mass-fraction and velocity fields in the compression chamber of a reciprocating-piston engine with injection and evaporation of liquid droplets is complex. Continuous models can be derived and solved using a Computation Fluid Dynamics (CFD) approach, to account for three-dimensional effects of such flows. In this study, a different modelling technique is used. The droplet motion and evaporation is determined with a discrete analysis described in section 2.3. A dynamic lumped-mass analysis is used to describe the heat and mass transfer to and from the gas, while the gas velocity field is assumed to be one-dimensional. The gas velocity distribution along the x-axis is taken to be linear (see Fig. 1):

$$\mathrm{v_g}(x,t) = \frac{x}{x_\mathrm{f}(t)} \mathrm{v_p}(t) \quad . \tag{1}$$

The liquid injection is triggered during the compression stroke (at a crank angle $\theta_\mathrm{inj} = 3\pi/2$) and any remaining droplets are assumed to be evacuated during the exhaust. If the droplets hit the piston head before then, a liquid film is formed (see Fig. 1). However, due to the small droplet diameters considered in this article (from 10 to 100 µm) and the low injection speed (0.5 m/s), the droplets quickly reach velocity equilibrium with the gas, and rarely come into contact with the cylinder walls.

2.1. Piston motion equations

In most reciprocating-piston engines, the piston motion is set by a rotating crankshaft, via a connecting rod. The piston motion equations for a given crankshaft rotational speed, ω, are given as functions of the crank angle, θ:

$$x_\mathrm{p}(\theta) = r_\mathrm{s}(1-\cos\theta) + L_\mathrm{cr}\left(1 - \sqrt{1 - \left(\frac{r_\mathrm{s}}{L_\mathrm{cr}}\right)^2 \sin^2\theta}\right) \quad \text{, and} \tag{2}$$

$$\mathrm{v_p}(\theta) = \omega \cdot \left(r_\mathrm{s}\sin\theta + \frac{{r_\mathrm{s}}^2 \cos\theta \sin\theta}{\sqrt{{L_\mathrm{cr}}^2 - {r_\mathrm{s}}^2 \sin^2\theta}} \right) \quad , \tag{3}$$

where L_cr is the connecting-rod length and r_s is the crankshaft radius.

2.2. Mass-lumped modelling of the gas phase

The compression chamber of a reciprocating-piston compressor with water-spray injection is filled with liquid droplets dispersed in the gas phase, composed of dry air and water vapour. The gas phase is treated as a lumped mass and the thermodynamic and transport properties of the humid air are derived from CoolProp [6]. The transient gas pressure and mass-averaged temperature are calculated throughout the cycle (expansion, intake, compression, spray injection and exhaust) using mass and energy conservation equations written for a control volume, V_g, that is the cylinder volume occupied by the gas phase.

2.2.1. Gas-phase conservation equations

Mass conservation equations

Several mass transfer processes occur in the compression chamber: intake and exhaust via the reed valves, and vapour formation from the evaporation of droplets. Two equations must be solved to determine the mass of the components of humid air: dry air (subscript a) and vapour (subscript v). Equations (4) and (5) are respectively the total mass and vapour mass conservation equations:

$$\frac{\mathrm{d}m_\mathrm{g}}{\mathrm{d}t} = \sum_{\mathrm{in/ex}} \dot{m}_\mathrm{in/ex} - \sum_{\mathrm{d}=1}^{N_\mathrm{d}} \dot{m}_\mathrm{d} \quad \text{, and} \tag{4}$$

$$\frac{\mathrm{d}m_\mathrm{v}}{\mathrm{d}t} = \sum_{\mathrm{in/ex}} Y_{\mathrm{v_{in/ex}}}\, \dot{m}_{\mathrm{in/ex}} - \sum_{\mathrm{d}=1}^{N_\mathrm{d}} \dot{m}_\mathrm{d} \qquad , \tag{5}$$

where m_g and m_v are respectively the total and vapour mass (with: $m_\mathrm{g} = m_\mathrm{a} + m_\mathrm{v}$), N_d is the number of droplets and Y_v is the mass fraction of vapour.

Energy conservation equation

The corresponding energy-conservation equation is:

$$m_\mathrm{g}\frac{\mathrm{d}h_\mathrm{g}}{\mathrm{d}t} = V_\mathrm{g}\frac{\mathrm{d}P}{\mathrm{d}t} + \dot{Q}_\mathrm{wg} - \sum_{\mathrm{d}=1}^{N_\mathrm{d}}\left[\dot{m}_\mathrm{d}\left(h_\mathrm{g,s} - h_\mathrm{g}\right) + \dot{Q}_\mathrm{gd}\right]_\mathrm{d} + \sum_{\mathrm{in/ex}} \dot{m}_{\mathrm{in/ex}}\left(h_{\mathrm{in/ex}} - h_\mathrm{g}\right) \qquad , \tag{6}$$

where h_g is the mass-lumped enthalpy of the gas. The mass flow rates $\dot{m}_{\mathrm{in/ex}}$ are positive for fluid flows into the compression chamber and negative for fluid leaving the chamber.

2.2.2. Gas flow through intake and exhaust valves

Conventional reciprocating-piston compressor valve-systems are made of reed plate valves, positioned in the cylinder head. Intake and exhaust flows through reed valves induce pressure oscillations both in the compression chamber and in the intake/exhaust ducts. For a careful study of these instabilities, flow equations in the ducts must be solved and the different vibration modes of the reed valves determined [7]. However, these transient effects are beyond the scope of the present study. The pressure in the intake and exhaust ports are thus set to be constant and only the fundamental vibration mode of the reed plate is accounted for. The valve flow area and mass flow rates are determined using the mathematical model proposed by Govindan et al. [8].

2.2.3. Gas-to-wall heat transfer

The irreversible unsteady gas-to-wall heat transfer in reciprocating engines is challenging to predict, as discussed by the authors in previous publications [9], [10]. To our knowledge, the most advanced correlations available for this in-cylinder heat transfer are those proposed by Lekic and Kok [11] and Kornhauser and Smith [12]. The latter is an empirical correlation developed for pressure ratios up to 4; it is used in this study because of the small pressure ratio ($P_\mathrm{ex}/P_\mathrm{in} = 3$) imposed on the compressor. This correlation is based on a complex Nusselt number to account for the phase shift between the instantaneous gas-to-wall heat transfer rate and temperature difference. Interested readers might refer to the review written by Prasad [13] where the in-cylinder heat transfer phenomena are well described.

2.3. Liquid-droplet evaporation

The analysis of water-spray cooling in reciprocating-piston compressors requires the simultaneous calculation of motion and evaporation rate of many individual droplets. In this first attempt to build a model accounting not only for conventional loss mechanisms (gas-to-wall heat transfer, pressure losses through the intake/exhaust valves) but also for the two-phase flow heat transfer with phase change, several simplifying assumptions have been made.

Regarding the direct spray injection, it is assumed that all droplets are injected at the same time and have the same radius and velocity (0.5 m/s), directed downwards along the *x*-axis, see Fig. 1. The droplet trajectories are determined with a one-dimensional analysis presented in section 2.3.3.

As discussed in [14], single-droplet evaporation models fall under two major categories: spherically-symmetric (e.g. the infinite-conductivity and the conduction-limit models) and axisymmetric models that take into consideration both inner- and outer-droplet convective effects. An extensive comparative study of these different models can be found in [15]. In the current study, the liquid-phase analysis uses the infinite-conductivity model, also called the ‘rapid mixing limit’, based on the assumption that the droplet temperature is spatially uniform though varies in time. The algorithm proposed by Abramzon and Sirignano [16] (initially developed for the vaporisation of fuel droplets in internal-combustion engines) is used for the gas-phase analysis at the droplet surface. This model is based on an extended version of the so-called film theory [17] that includes the effects of the Stefan flow on the heat and mass transfer at the surface of the droplet, which tend to increase the thickness of thermal and mass boundary layers.

2.3.1. Single-droplet evaporation rate

The droplet-evaporation rate is driven by the local mass-fraction difference near the droplet surface. Abramzon and Sirignano [16] propose the following expression for the instantaneous droplet evaporation rate:

$$\dot{m}_{\mathrm{d}} = -\,\pi D_{\mathrm{d}} \overline{\rho_{\mathrm{g}}}\,\overline{\mathcal{D}_{\mathrm{g}}} \mathrm{Sh}^{*} \ln(1+B_{\mathrm{m}}) \quad , \tag{7}$$

where Sh^* is the corrected Sherwood number obtained with the Frossling correlations, corrected by a factor dependent on the Spalding mass transfer number, B_{m} [16]:

$$B_{\mathrm{m}} = \frac{Y_{\mathrm{v,s}} - Y_{\mathrm{v}}}{1 - Y_{\mathrm{v,s}}} \quad . \tag{8}$$

The value Y_{v} is the vapour mass fraction in the bulk humid air, while $Y_{\mathrm{v,s}}$ is that at the droplet surface, where the air is saturated (relative humidity of 100 %) at the droplet surface temperature (see Fig. 1).

2.3.2. Droplet heat transfer

The instantaneous heat transfer between the droplet and the surrounding gas influences the vaporisation rate. Given the small size of the injected droplets (from 10 to 100 µm), the infinite-conductivity model seems appropriate and has been chosen for this preliminary study. A further analysis of the conjugate heat transfer would be required to determine the most appropriate liquid-heating model to be chosen for spray injection in piston compressors.

As previously noted, the droplet temperature is uniform but transient. The following energy-conservation equation is solved to determine the heat transferred to the droplet and its temperature:

$$m_{\mathrm{d}} c_{\mathrm{p,d}} \frac{dT_{\mathrm{d}}}{dt} = \dot{Q}_{\mathrm{gd}} + \dot{m}_{\mathrm{d}} \Delta h_{\mathrm{vap}} \quad , \tag{9}$$

where $\dot{Q}_{\mathrm{gd}}$ is the instantaneous convective heat flow rate from the gas to the droplet, obtained with:

$$\dot{Q}_{\mathrm{gd}} = -\,\dot{m}_{\mathrm{d}} \frac{\overline{c_{\mathrm{p,g}}}}{B_{\mathrm{t}}} \left(T_{\mathrm{g}} - T_{\mathrm{d}}\right) \quad . \tag{10}$$

B_{t} is the Spalding thermal transfer number, obtained from the Spalding mass transfer number B_{m} and the Nusselt number [16].

2.3.3. Droplet velocity

The droplet motion is expected to be governed by viscous effects and gravity. This assumption is justified by the high density ratio between the droplet water and the surrounding humid air. The drag force is acting opposite to the relative velocity of the droplet, $\mathrm{w} = \mathrm{v_d} - \mathrm{v_g}$. The droplet motion equation is thus written:

$$m_{\mathrm{d}} \frac{\mathrm{d}v_{\mathrm{d}}}{\mathrm{d}t} = 3\pi D_{\mathrm{d}} \mu_{\mathrm{g}} K_s \left(\mathrm{v_g} - \mathrm{v_d}\right) + m_{\mathrm{d}} \mathrm{g} \quad , \tag{11}$$

where K_s is the Stokes correction factor that accounts for real-flow effects around the droplet. For fixed-diameter spherical objects, Kersey et al. [18] propose an empirical correlation to estimate K_s as a function of the droplet Reynolds number $\mathrm{Re_d}$:

$$K_s^o = 1 + \frac{\mathrm{Re_d}}{4\left(1+\sqrt{\mathrm{Re_d}}\right)} + \frac{\mathrm{Re_d}}{60} \quad . \tag{12}$$

However, the Stefan flow at the droplet surface reduces the drag force. This effect is accounted for through a semi-empirical correction proposed by Sirignano [19]:

$$K_s = \frac{K_s^o}{1 + B_\mathrm{m}} \quad . \tag{13}$$

2.4. Numerical methods

The set of equations (1-13) are solved with an object-oriented code implemented in Matlab. First, the gas velocity is given by (1). For each time step, the motions of droplets are obtained by solving the momentum-conservation equation (11) for each drop using the droplets characteristics at the previous time step. Then, the droplets evaporation rates and the gas flow rate through intake and exhaust valves are determined explicitly, i.e. based on the state of the system at the previous time step. This allows to solve the mass-conservation equations and determine the mass and humidity ratio in the gas phase as well as the droplet diameters. The energy-conservation equations, namely (6) and (9), are then solved implicitly and simultaneously using the Trust-Region Dogleg method implemented in the *fsolve* function of Matlab [20].

3. Results and discussion

This paper focuses on the influence of initial droplet diameter and injected mass upon the efficiency of a CAES system. A performance metric for the efficiency of such a system needs to measure the amount of recoverable energy after storage versus the energy spent during the storage process. We propose the compression-storage efficiency, η (hereinafter referred in short as compression efficiency), defined as the ratio between the maximum specific work that can be recovered after storage, w_st, and the compression specific work, w_c:

$$\eta = \frac{w_\mathrm{st}}{w_\mathrm{c}} \quad . \tag{14}$$

In calculating the maximum specific-work output, w_st, it is assumed that the compressed gas is stored for long enough to reach ambient temperature (set to $T_\mathrm{atm} = 25$ °C), resulting in an effective storage pressure, P_st (lower than the compressor-exhaust pressure, P_ex). It is then expanded isothermally, yielding the following expression for the recoverable specific-energy for a steady-flow process:

$$w_\mathrm{st} = \frac{P_\mathrm{st}}{\rho_\mathrm{ex}} \ln\left(\frac{P_\mathrm{st}}{P_\mathrm{atm}}\right) \quad , \tag{15}$$

where ρ_ex is the mean density at the exhaust of the compressor.

As in the study of liquid-piston compressor efficiency by Qin and Loth [5], the influence of the injected mass of water droplets is measured with the mass-loading parameter, τ, defined as the ratio of the injected liquid mass, m_inj, to the mass of humid air drawn from the suction line, m_in:

$$\tau = \frac{m_\mathrm{inj}}{m_\mathrm{in}} \quad . \tag{16}$$

3.1. Operating conditions

Many operating conditions (such as the injection strategy, RPM, and exhaust pressure) are to be varied to determine their influence on the compressor behaviour. However, only the injected mass and droplet diameter are varied in the present parametric study. Droplet diameters of between 10 and 100 µm are considered here, as these are readily achieved by existing diesel injector nozzles. A low pressure ratio and rotational speed of 100 RPM was chosen to assist with validation by future experimental work, with the latter helping to ensure full evaporation of the droplets. The dimensions and operating conditions of the spray-cooled compressor are summarised in Table 1. It must be emphasised that the compressor dimensions are chosen only as an illustrative example, and are not representative of an optimised design for industrial CAES applications.

Table 1. Compressor dimensions and operating conditions

Parameter	Symbol	Value
Shaft radius	r_{s}	39 mm
Connecting rod length	L_{cr}	148.5 mm
Piston bore diameter	D_{b}	105 mm
Dead volume height	L_{dv}	14 mm
Rotation Per Minute	RPM	100
Injection crank angle	θ_{inj}	$3\pi/2$ (mid-stroke)
Injection temperature	T_{inj}	25 ˚C
Exhaust pressure	P_{ex}	3 bar
Intake pressure	P_{in}	1 bar
Droplet diameter	D_d	[10,100] µm
Injected mass	m_{inj}	[0,100] mg

3.2. Instantaneous heat and mass transfer

In this section, a single spray-injection configuration ($m_{\mathrm{inj}} = 5$ mg and $D_{\mathrm{inj}} = 10$ µm) is compared to the baseline case without spray injection to investigate the heat and mass transfer processes between the droplets and the surrounding gas.

Fig. 2 shows the indicated pressure-volume (P-V) diagram and the temperature-volume (T-V) trace for both configurations. Using these diagrams, the effects of spray cooling on the power consumption and on the mean exhaust temperature can be described qualitatively and measured quantitatively.

On the P-V diagram in Fig. 2(a), the pressure losses through the reed valves can be seen as a difference between the suction pressure and the compression chamber (for intake), and the compression chamber and discharge pressure (for exhaust). The P-V traces are similar for both configurations up until spray injection takes place. The injection of water droplets cools down the gas, thus reducing its pressure in comparison with the baseline compression. The decrease in the P-V slope during the compression stroke indicates that the compression process tends toward an isothermal compression due to the cooling effect of the droplet spray. The spray cooling-effect is here beneficial as it reduces the compression work (which can be measured by the area enclosed within the P-V trace). At 100 RPM, the power required in the baseline case is 112.7 W and falls to 107.3 W with spray injection, corresponding to a 4.8 % reduction.

On the T-V diagram in Fig. 2(b), the influence of droplets is even more obvious. The entire T-V trace is shifted down to lower temperatures. The mean cyclic temperature of the cycle is thus lower, as is the discharge temperature, which falls from $T_{\mathrm{ex}}^{\mathrm{o}} = 404.6$ K for the baseline case to $T_{\mathrm{ex}}^{*} = 371.8$ K with spray cooling. The decrease in the stored gas temperature is beneficial for isothermal-type CAES applications as less energy will be lost in the form of heat rejection to the environment during storage and prior to energy recovery. The reduced exhaust temperature therefore ensures a higher recoverable energy after storage.

The gain in recoverable energy and the decrease in compression power offered by liquid-spray cooling are both measured by the compression-storage efficiency, η, defined in (14). The efficiency increases significantly, from $\eta = 49.6$ % for the baseline case to $\eta = 57.6$ % for the injection conditions studied in this section. This represents a 16.1 % relative increase in compression efficiency, accounting for both the gain in recoverable energy and the decrease in compression power.

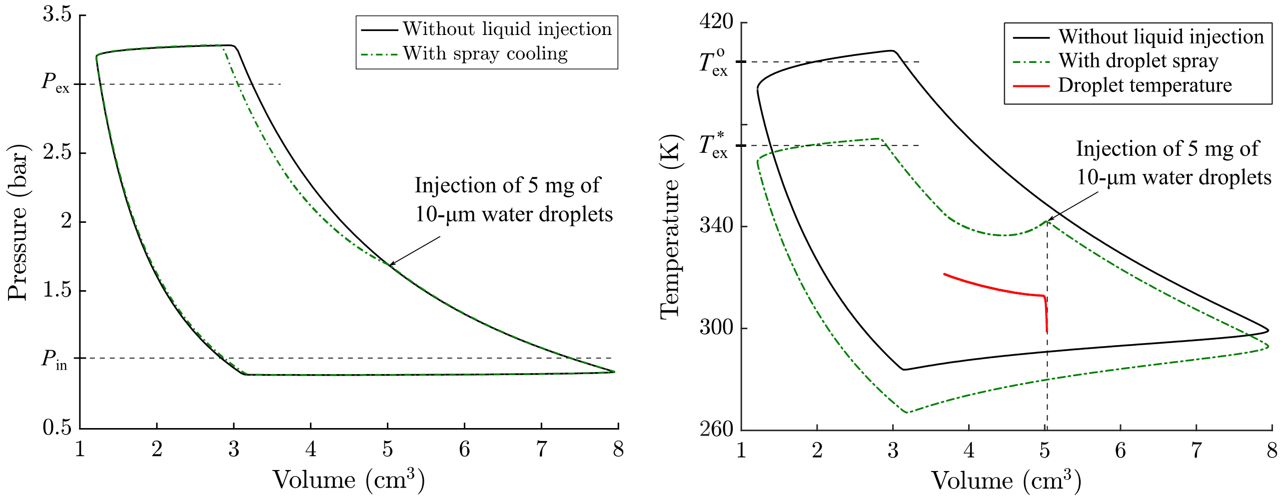

(a) *(b)*

Fig. 2. a) Pressure-volume and b) temperature-volume traces for humid air compressed from P_{in} = 1 atm to P_{ex} = 3 bar with and without the injection of 5 mg of 10-µm water droplets.

Fig. 2(b) also shows the temperature evolution of a single droplet alongside the gas temperature. It is observed that the transient behaviour is captured well and that the droplet fully evaporates before the exhaust valves open. In this very case, all the water spray vaporises before the exhaust stroke, which is not always the case, as will be observed later.

3.3. Benefits of liquid injection for CAES

To measure the benefits of liquid injection for CAES and determine the optimal injection strategy, a parametric study is proposed to characterise the influence of the mass of injected water and of the droplet diameter on the compression efficiency.

Fig. 3(a) shows the dependency of the compression efficiency, η, upon both the injected mass of water droplets and their diameter. For a given mass loading, smaller droplet represents a higher gas-liquid interface area and thus a higher cooling capacity of the spray. Smaller droplets therefore tend to decrease the required compression power and increase the energy that can be efficiently stored. Higher efficiency is reached with lower-diameter droplets for the range of mass loadings presented in Fig. 3(a).

For a given droplet diameter, increasing the mass loading also leads to an increase in efficiency, as expected. However, for the 10-µm droplets, it is apparent that a plateau is reached for mass loadings exceeding 5 %. This reflects the fact that for high mass loadings, not all the droplets are fully evaporated before the exhaust stroke. A significant part of the injected mass is drawn from the compression chamber when the exhaust valves open. A new parameter, called effective mass loading, τ_{eff}, is defined as the ratio of the mass of water vaporised in the chamber, m_{vap}, to the mass of humid air drawn from the suction line:

$$\tau_{\mathrm{eff}} = \frac{m_{\mathrm{vap}}}{m_{\mathrm{in}}} \quad . \tag{17}$$

Fig. 3(b) shows the same results plotted against the effective mass loading, independent of droplet diameter. The effective mass loading is seen to vary much less than the basic mass loading between the scenarios considered. The compression efficiency correlates well with this new parameter τ_{eff}, which is representative of the amount of heat transferred from the gas to the droplets. Indeed, as observed in Fig. 2(b), the droplet temperature increase immediately after injection is very steep. Subsequently, most of the interfacial droplet-to-gas heat transfer is balanced by the droplet vaporisation: the heat penetrating into and heating up the liquid is small in comparison with the overall gas-to-liquid heat flow.

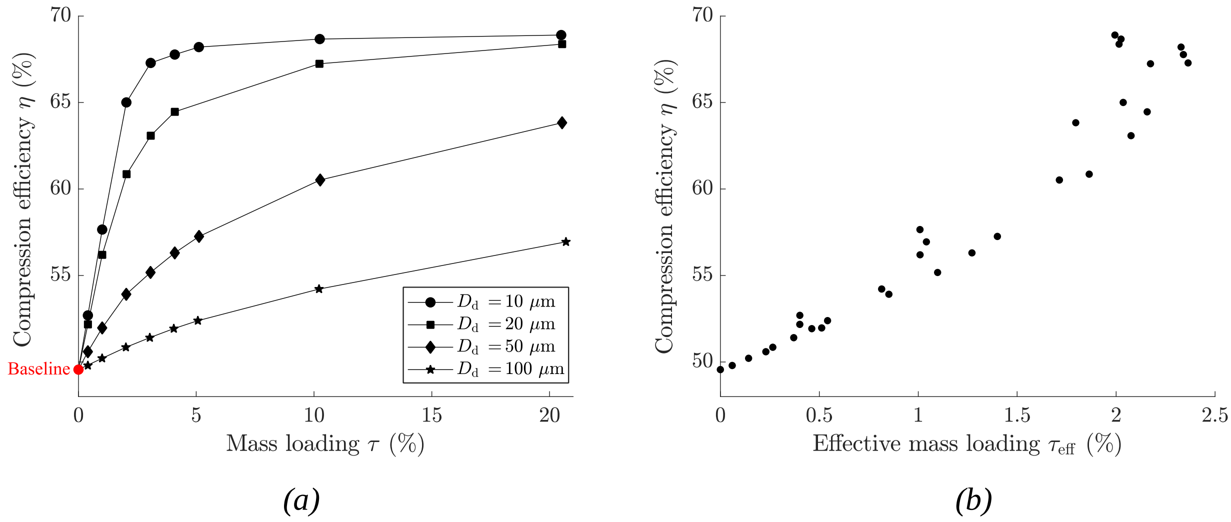

Fig. 3. a) Compression-storage efficiency as a function of mass loading for various droplet diameters. b) Compression-storage efficiency as a function of effective mass loading.

These observations show evidence of the benefits of water-spray injection for CAES applications. The maximum relative increase in compression-storage efficiency observed in this parametric study is 39 % (from 49.6 % for the baseline case to 68.9 % for the most efficient system). Direct injection of droplet spray requires the upstream ambient-temperature water tank to be at higher pressure than that of the compression chamber, with a greater pressure difference required for smaller droplet diameters. A trade-off must therefore be made between the energy savings with direct injection and the power required to provide spray-cooling.

4. Conclusions and perspectives

In this paper, a dynamic model of droplet-spray vaporisation in reciprocating-piston compressors is presented. It accounts for all the major loss mechanisms encountered in these engines, including the pressure losses through the valves and the irreversible thermal losses due to the gas-to-wall heat transfer. It is based on a lumped-mass analysis of the gas phase (humid air) and a discrete analysis of the droplets. The vaporisation of the liquid spray is predicted using the model proposed by Abramzon and Sirignano [16] and the 'rapid mixing limit' hypothesis is made to calculate the transient droplet temperature. This model provides time-resolved description of the heat and mass transfer in the compression chamber. It is used to assess the potential benefits of water-droplet spray injection for Compressed Air Energy Storage (CAES) technologies.

The results indicate that the injection of liquid-water spray during the compression is beneficial for isothermal CAES applications. The decrease in compressor delivery temperature ensures a higher overall efficiency of the CAES system, since it reduces the quantity of heat rejected to the environment. The effect is enhanced with low-diameter droplets that offer a higher exchange area for the same injected mass. The maximum relative increase in compression-storage efficiency observed in this parametric study is 39 % (from an efficiency of 49.6 % for the baseline case to 68.9 % for the most efficient system).

However, for a fair comparison between the baseline case and water-cooled compression processes, it is important to account for the energy expended (and cost) in providing such a cooling effect. A further study of the liquid injector and the pressure losses through the injection nozzles would allow definitive conclusions to be drawn. Furthermore, a techno-economic analysis would be necessary to assess potential benefits for CAES applications. The simulation tool presented in this paper is a first step towards a full assessment of this potential.

In future works, additional operating conditions (such as the injection strategy – e.g. the injection crank angle, RPM, pressure ratio) will be varied to assess their influence on the compressor behaviour. Moreover, the droplet-spray characteristics (geometry and diameter distributions for example) are important factors in the atomisation. A specific effort will be made to improve the analysis of the spray dynamics. Finally, CFD modelling of the liquid spray – and more generally of two-phase flows in reciprocating-piston engines – will be undertaken to refine the results of the lumped-mass analysis and assess the influence of turbulent flows.

Nomenclature

B	Spalding transfer number
c_p	isobaric specific heat capacity, J/(kg K)
D	diameter, m
$\mathcal{D}$	binary diffusion coefficient, m^2/s
h	specific gas enthalpy, J/kg
Δh_{vap}	specific latent heat of vaporisation, J/kg
K_s	Stokes correction factor
L	length, m
m	mass of gas in the control volume, kg
$\dot{m}$	mass flow rate, kg/s
N_d	number of droplets
P	pressure, Pa
$\dot{Q}$	heat flow rate, W
R	specific gas constant, J/(kg K)
r	radius, m
Re	Reynolds number
Sh	Sherwood number
t	time, s
T	temperature, K
v	velocity, m/s
V	volume, m^3
w	specific energy / work, J/kg
x	x-axis position, m
Y	mass fraction

Greek characters

η	compression-storage efficiency
θ	crank angle, rad
ρ	density, kg/m^3
τ	mass loading
ω	angular frequency, rad/s

Subscripts

a	dry air
b	bore
d	droplet
dv	dead volume
ex	exhaust
eff	effective
f	liquid film
g	gas (humid air)
in	intake
inj	injection
m	mass
s	surface
st	storage
t	thermal
v	vapour
w	wall

References

[1] Knecht W., Some Historical Steps in the Development of the Common Rail Injection System. Transactions of the Newcomen Society 2004;74(1):89-107.

[2] BMW. BMW Concept M4 GTS. 2016.

[3] Centre for Low Carbon Futures. Liquid Air on the Highway. 2014.

[4] Coney M.W., Stephenson P., Malmgren A., Linnemann C., Morgan R.E., Richards R.A., Huxley R., Abdallah H., Development Of A Reciprocating Compressor Using Water Injection To Achieve Quasi-Isothermal Compression. In: Proceedings of the International Compressor Engineering Conference; 2002.

[5] Qin C., Loth E., Liquid piston compression efficiency with droplet heat transfer. Applied Energy 2014;114:539-550.

[6] Bell I.H., Wronski J., Quoilin S., Lemort V., Pure and Pseudo-pure Fluid Thermophysical Property Evaluation and the Open-Source Thermophysical Property Library CoolProp. Industrial & Engineering Chemistry Research 2014;53(6):2498-2508.

[7] Soedel W., Sound and vibrations of positive displacement compressors. USA: CRC Press; 2006.

[8] Govindan N., Jayaraman V., Venkatasamy R.S., Ramasamy M., Mathematical modeling and simulation of a reed valve reciprocating air compressor. Thermal science 2009;13(3):47-58.

[9] Simpson M., Rotolo G., Sapin P., De Palma P., White A.J., Markides C.N., Thermodynamic performance maps of reciprocating-piston expanders for operation at off-design and part-load conditions. In: Proceedings of the 13th International Conference on Heat Transfer, Fluid Mechanics and Thermodynamics; 2017; Portorož, Slovenia.

[10] Sapin P., Taleb A., Barfuss C., White A.J., Fabris D., Markides C.N., Thermodynamic Losses in a Gas Spring: Comparison of Experimental and Numerical Results. In: Proceedings of the 12th International Conference on Heat Transfer, Fluid Mechanics and Thermodynamics; 2016; Malaga, Spain.

[11] Lekic U., Kok J.B.W., Heat transfer and fluid flows in gas springs. Open Thermodynamics Journal 2010;4:13-26.

[12] Kornhauser A.A., Smith J.L., Application of a complex Nusselt number to heat transfer during compression and expansion. Journal of heat transfer 1994;116(3):536-542.

[13] Prasad B.G., Heat transfer in reciprocating compressors - a review. In: Proceedings of the International Compressor Engineering Conference; 1998; Purdue, USA.

[14] Aggarwal S.K., Sirignano W.A., Tong A.Y., A comparison of vaporization models in spray calculations. 1984;22(10):1448-1457.

[15] Sazhin S.S., Modelling of fuel droplet heating and evaporation: Recent results and unsolved problems. Fuel 2017;196:69-101.

[16] Abramzon B., Sirignano W.A., Droplet vaporization model for spray combustion calculations. International journal of heat and mass transfer 1989;32(9):1605-1618.

[17] Bird R.B., Stewart W.E., Lightfoot E.N., Transport phenomena. Madison, USA; 1960.

[18] Kersey J., Loth E., Lankford D., Effect of evaporating droplets on shock waves. AIAA journal 2010;48(9):1975-1986.

`[19] Sirignano W., Fluid dynamics and transport of droplets and sprays. Cambridge, UK: Cambridge university press; 1999.

[20] Powell M.J.D., A Fortran subroutine for solving systems of nonlinear algebraic equations. In: Rabinowitz P., Numerical methods for nonlinear algebraic equations. 1970. p. 150-166.